Variational method combined with Frangi vesselness for tubular object segmentation

Olivia Miraucourt, Anna Jezierska, Hugues Talbot, Stéphanie Salmon, Nicolas Passat

VARIATIONAL METHOD COMBINED WITH FRANGI VESSELNESS FOR TUBULAR OBJECT SEGMENTATION

O. Miraucourt[1,2], A. Jezierska[2], H. Talbot[2], S. Salmon[1], and N. Passat[1]

[1]Laboratoire de Mathématiques EA 4535 & CReSTIC EA 3804, Université de Reims Champagne-Ardenne, UFR Sciences Exactes et Naturelles, Moulin de la Housse - BP 1039, 51687 Reims CEDEX 2, France, `olivia.miraucourt,stephanie.salmon,nicolas.passat@univ-reims.fr`
[2]Laboratoire d'Informatique Gaspard-Monge UMR 8049, Université Paris-Est, Cité Descartes, Bâtiment Copernic, 5 bd Descartes Champs sur Marne - 77454 Marne-la-Vallée CEDEX 2, France, `anna.jezierska,hugues.talbot@esiee.fr`

SUMMARY

Tubular structure extraction from (bio)medical images is a prerequisite for many applications in bioengineering. The two main issues related to such extraction, namely denoising and segmentation, are generally handled independently and sequentially, by dedicated methods. In this article, we model the problem of tubular structure extraction in an optimization framework and we show how a Hessian-based vesselness measure can be embedded in the formulation, allowing in particular robust vessel extraction. Preliminary experiments of this method, on synthetic and retinal images, emphasise the potential usefulness of this approach.

Key words: *tubular structures, Frangi vesselness, total variation, primal-dual algorithm*

1 CONTEXT

Extraction of tubular structures (vessels, neurones, fibres, ...) is a mandatory but challenging task for many biomedical applications, especially in angiographic image analysis [1]. The difficulty first derives from the size of such thin objects, that are generally a few pixel thick. In addition to their complex geometric properties (thin, long, curvilinear), the visualization of these objects is also often corrupted by noise. In this article, we consider a model that can handle the two induced issues, namely (i) denoising and (ii) enhancement / segmentation.

More precisely, our strategy relies on the variational approach, that was proved successful in general problems of image denoising and segmentation. Mathematically speaking, denoising is an ill-posed inverse problem; to convert it into a well-posed problem, we can impose some regularity on the solution. To this end, Tikhonov used a quadratic regularization of the solution, which removes the noise; however, this results in strong blurring effects. In 1992, Rudin, Osher and Fatemi (ROF) replaced this quadratic regularization with a L^1 norm, called *total variation* that preserves edges [2]. When the L^2 data term in the ROF model is replaced with an L^1 norm, we obtain the so-called TV-L^1 model but the difference between both models remains marginal [3]. We can solve the ROF and TV-L^1 problems efficiently, by using the primal-dual algorithm (Sec. 2.1).

The eigenvalue analysis of the Hessian matrix is currently considered as the gold-standard to capture the a priori information about tubular structures location. More precisely, the eigenvalues characterize the local geometry (tubular, plane, blob) and contrast (dark or bright). Different combinations of these eigenvalues, called *vesselness* functions, were proposed to enhance points likely to belong to the vessels [4, 5]. Among these measures, Frangi vesselness was experimentally assessed as the most relevant to characterize vessels of different sizes via a scale-space approach [6]. We propose to include, for the first time, this vesselness in the ROF and TV-L^1 models (Sec. 2.2) and we present preliminary results for 2D synthetic images and 2D retinal images (Sec. 3).

This work is part of the project VIVABRAIN[1], whose final objective is to compute virtual cerebral angiography images. In this context, our method constitutes one of the very first steps of a methodological pipeline that aims to reconstruct cerebral vascular networks from medical images, in order to generate 3D anatomical models (computational meshes) and further simulate the flowing blood [7] and subsequent virtual magnetic angiography acquisitions.

2 METHODOLOGY

First, let us recall that the ROF model corresponds to the following optimization problem:

$$\min_x \int_{\mathbb{R}^N} |\nabla x| + \frac{\lambda}{2} \int_{\mathbb{R}^N} (x - f)^2 dx \qquad (1)$$

where x is the denoised image, f is the observed image and λ is a parameter used to handle the trade-off between the regularization term (on the left) and the data fidelity term (on the right). This data fidelity term ensures that the denoised image remains close to the observed image. When the L^2 data term in the ROF model is modified by considering the L^1 norm, we obtain the so-called TV-L^1 model, that corresponds to the following optimization problem:

$$\min_x \int_{\mathbb{R}^N} |\nabla x| + \lambda \int_{\mathbb{R}^N} |x - f| dx \qquad (2)$$

In the following, we present the primal-dual algorithm, that allows us to solve the two convex problems (1) and (2).

2.1 Optimization approach

Let $F \in \Gamma_0(\mathbb{R}^N)$, $G \in \Gamma_0(\mathbb{R}^M)$ and $K : \mathbb{R}^N \to \mathbb{R}^M$ be a continuous, linear operator, where $\Gamma_0(\mathbb{R}^N)$ is the class of proper, convex, lower-semicontinuous functions from $\mathbb{R}^N$ to $]-\infty, +\infty]$. The general formulation of the considered problem is given by:

$$\min_{x \in \mathbb{R}^N} F(Kx) + G(x) \qquad (3)$$

This minimization problem can be efficiently solved by using various convex optimizations tools, such as proximal splitting algorithms (see [8] for a survey). These methods proceed by *splitting* the objective function to minimize (which is not necessarily differentiable) into simpler functions that are dealt with individually. The name *proximal* arises from the fact that each non-smooth function is handled via its proximity operator. The use of such proximity operator is computationaly efficient, since the explicit form of this operator exists.

Definition 1 *Let $F \in \Gamma_0(\mathbb{R}^N)$. For every $x \in \mathbb{R}^N$, the minimization problem:*

$$\min_{y \in \mathbb{R}^N} F(y) + \frac{1}{2} \|x - y\|^2 \qquad (4)$$

admits a unique solution, which is denoted by $\mathrm{prox}_F x$. The so-defined operator $\mathrm{prox}_F : \mathbb{R}^N \to \mathbb{R}^N$ is the proximity operator *of F.*

We chose the primal-dual algorithm proposed in [9], which can be easily implemented. Consider Eq. (3); using the Fenchel-Moreau theorem, it can be reformulated as the saddle-point problem:

$$\min_{x \in \mathbb{R}^N} \max_{y \in \mathbb{R}^M} \langle Kx, y \rangle + G(x) - F^*(y) \qquad (5)$$

where $F^*(y) = \sup_{x \in \mathbb{R}^N} \langle p, x \rangle - F(x)$ is the Legendre-Fenchel conjuguate. The key-idea is then to alternate gradient descent in x and gradient ascent in y. The induced algorithm is summarized in Alg. 1; its convergence with rate $\mathcal{O}(1/N)$ is proved in [9].

Algorithm 1: Primal-dual algorithm for solving Eq. (3)

Choose $\rho, \tau > 0$, $\theta \in [0,1]$, $(x_0, y_0) \in \mathbb{R}^N \times \mathbb{R}^M$ and set $\overline{x}_0 = x_0$.
for $n = 0, 1, \ldots$ **do**

$\quad y_{n+1} = \text{prox}_{\rho F^*}(y_n + \rho K \overline{x}_n)$
$\quad x_{n+1} = \text{prox}_{\tau G}(x_n - \tau K^T y_{n+1})$
$\quad \overline{x}_{n+1} = x_{n+1} + \theta(x_{n+1} - x_n)$
end

2.2 Frangi vesselness

Frangi *et al.* proposed a vesselness function $\mathcal{V}_0(x)$ which uses the eigenvalues γ_i of the Hessian matrix to discriminate vessel structures [6]. Eigenvalue analysis can be performed on the Hessian matrix, in order to extract one or more principal directions of the local structure of the image. Compared with the image gradient, whose response is independent of the shape and local structures of boundaries, the Hessian matrix can capture the shape characteristics of objects, such as tubes, planes, blob surfaces or noise. For an ideal tubular structure in 3D, we have $\gamma_3 \approx \gamma_2 \gg \gamma_1 \approx 0$. The vesselness measure is then defined via three heuristic, exponential functions of eigenvalues, to discriminate the various kinds of structures. In order to provide a relevant result in a wide range of line sizes, the filter is applied at different scales, σ (standard-deviations), by considering Gaussian scale-space analysis. The maximal response is finally chosen within these multiple scales, providing information on the vessel size.

Hence, we propose to combine the proposed data fidelity term in Eq. (1) and Eq. (2) with vesselness prior. For that purpose, we replace the coefficient λ by:

$$\lambda = \alpha \lambda_{reg} + (1 - \alpha)\mathcal{V}_0(x) \tag{6}$$

where $\alpha \in [0,1]$ is a free parameter which balances the regularization and the vesselness (if $\alpha \approx 0$, we promote the vesselness whereas if $\alpha \approx 1$, we promote the regularization). The parameter λ – that was previously a constant value over the whole image – now locally depends on the Hessian analysis in each point, but the problem remains convex.

3 RESULTS AND OUTLOOK

In our first experiment, we tested the ROF model on a synthetic 2D image representing simple lines (Fig. 1(a–b)). For the ROF model, we have $F(Kx) = |\nabla x|$ and the proximity operator for the dual update F^* reduces to pointwise Euclidean projection onto the unit ball. The proximity operator for the primal update $G(x)$ is given in [9]. The algorithm is parametered by $\alpha = 0.5, \lambda_{reg} = 16$ and $\sigma \in [1,3]$. We compare the simple ROF model (Fig. 1(c)) with the hybrid ROF+vesselness model (Fig. 1(d)). We can notice that when we include the vesselness, the noise is better suppressed while lines are preserved.

For real data tests, we use images from the DRIVE[2] database (green channel version). Only the results for the TV-L^1+vesselness model are shown. The different parameters are $\alpha = 0.3$ or 0.7, $\lambda_{reg} = 2$ and $\sigma \in [1,5]$. We can remark that our model enhances vessels; in addition the smaller α, the better we denoise (Fig. 2(e)); while the higher α, the better details are preserved (Fig. 2(f)). Finally, we observe that our model does not explicitly segment, but it mainly enhances the tubular structures. To fix that issue, we are aiming to include the Chan-Vese model to the data term, as we already did in our previous work [10]. By combining these two models, we expect to avoid disconnections observed, for instance, in Fig. 2(c).

REFERENCES

[1] O. Tankyevych, H. Talbot, N. Passat, M. Musacchio and M. Lagneau. Angiographic image analysis. *Medical Image Processing: Techniques and Applications*, 115–144, Springer, 2011.

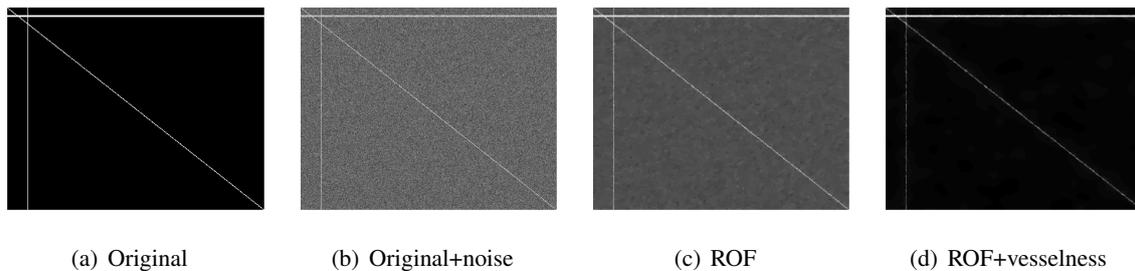[2] www.isi.uu.nl/Research/Databases/DRIVE

| (a) Original | (b) Original+noise | (c) ROF | (d) ROF+vesselness |

Figure 1: Synthetic 2D image results.

| (a) Original | (b) Ground truth | (c) [10] |

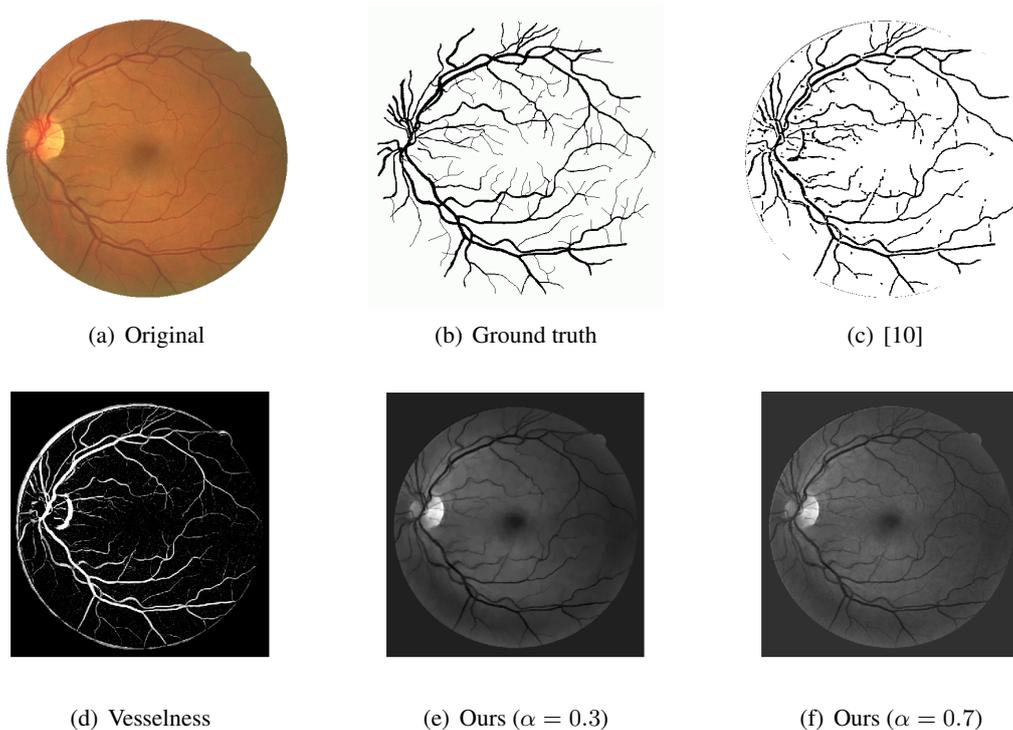| (d) Vesselness | (e) Ours ($\alpha = 0.3$) | (f) Ours ($\alpha = 0.7$) |

Figure 2: DRIVE database visual result.

[2] L.I. Rudin, S. Osher and E. Fatemi. Nonlinear total variation based noise removal algorithms. *Physica D: Nonlinear Phenomena*, 60(1–4):259–268, 1992.

[3] S. Alliney. Digital filters as absolute norms regularizers. *IEEE Transactions on Signal Processing*, 40(6):1548–1562, 1992.

[4] C. Lorenz, I.-C. Carlsen, T.M. Buzug, C. Fassnacht and J. Weese. Multi-scale line segmentation with automatic estimation of width, contrast and tangential direction in 2D and 3D medical images. *CVRMed-MRCAS – Lecture Notes in Computer Science*, 1205:233–242, 1997.

[5] Y. Sato, S. Nakajima, N. Shiraga, H. Atsumi, S. Yoshida, T. Koller, G. Gerig and R. Kikinis. Three-dimensional multiscale line filter for segmentation and visualization of curvilinear structures in medical images. *Medical Image Analysis*, 2(2):143–168, 1998.

[6] A.F. Frangi, W.J. Niessen, K.L. Vincken and M.A. Viergever. Multiscale vessel enhancement filtering. *MICCAI – Lecture Notes in Computer Science*, 1496:130–137, 1998.

[7] O. Miraucourt, O. Génevaux, M. Szopos, M. Thiriet, H. Talbot, S. Salmon, N. Passat. 3D CFD in complex vascular systems: A case study. *ISBMS – Lecture Notes in Computer Science*, 8789:86–94, 2014

[8] P.L. Combettes and J.-C. Pesquet. Proximal splitting methods in signal processing. *Fixed-Point Algorithms for Inverse Problems in Science and Engineering*, 185–212, Springer, 2011.

[9] A. Chambolle and T. Pock. A first-order primal-dual algorithm for convex problems with applications to imaging. *Journal of Mathematical Imaging and Vision*, 40(1):120–145, 2011.

[10] A. Jezierska, O. Miraucourt, H. Talbot, S. Salmon and N. Passat. A non-local Chan-Vese model for sparse, tubular object segmentation. *International Conference on Image Processing*, 907–911, 2014.